

双孔微剪切评定焊接接头的局部强度

蔡淑娟, 朱 亮, 张忠发

(兰州理工大学 省部共建有色金属先进加工与再利用国家重点实验室, 兰州 730050)

摘 要: 提出一种评价力学性能不均匀焊接接头强度的方法, 研制了测量材料局部力学性能的双孔微剪切试验装置, 对焊接接头各区域进行微剪切试验. 记录加载过程中载荷传感器和位移传感器传输的数据, 转化得到剪切应力-应变曲线. 建立双孔微剪切试验的有限元模型, 选择不同屈服应力和加工硬化指数的材料进行有限元模拟, 建立试验剪切应力-应变曲线与材料强度参数的相关性, 并利用拉伸试验对其准确性进行了验证. 结果表明, 利用双孔微剪切试验曲线可直接得到材料的强度参数, 并利用双孔微剪切试验测定 X70 管线钢焊接接头上各区的强度.

关键词: 双孔微剪切试验; 有限元模拟; 屈服强度; 抗拉强度

中图分类号: TG 407 文献标识码: A 文章编号: 0253-360X(2016)04-0043-04

0 序 言

焊接接头存在不均匀的力学性能, 焊接时母材局部受焊接热循环作用, 使沿焊缝横截面方向的温度分布极不均匀, 致使焊缝、热影响区(HAZ)与母材组织性能有较大差别. 即使是在窄小的 HAZ 内, 组织性能也很不均匀^[1]; 另外工程上为了某些需要, 有意识地采取非等强匹配的焊接接头. 对于热影响区软化的细晶粒钢焊接接头, 为了不损失整个接头的承载能力, 在设计上采用高匹配的焊接接头. 低匹配焊接接头常用于高强钢的焊接结构, 目的是为了减小冷裂纹倾向, 降低预热温度以降低焊接成本^[2,3]. 焊接接头的力学性能不均匀对接头承载能力有复杂的影响, 用有限元法对接头进行试验研究和分析时, 需要输入各个区域的强度, 其中最基本的参数有屈服强度和抗拉强度. 常规的试验方法, 例如在实际焊接接头上进行的热模拟试验以及缺口冲击或拉伸等力学性能试验, 难以准确获得焊接接头各区域局部力学性能的梯度变化及分布情况^[4,5]. LaVan^[6]用特殊的线切割方法切取微型拉伸试样, 在特制材料测试试验机上, 利用微拉伸法获得接头微区的应力应变关系, 得到可靠的试验数据, 但制样过程复杂. Zhang 和 Dom^[7]用微剪切试验直接给出焊接接头的强度分布数值, 但微剪试验中剪切时刀容易钝化, 直接影响了结果的准确性.

双孔微剪切法通过测试两孔之间材料的变形特

性来分析材料局部的力学性能^[8]. 无需制备小试样, 在被测试样区域打两盲孔, 直接进行剪切试验, 测定了焊接接头局部强度. 但双孔直径尺寸太小引起试验数据误差大.

文中在双孔微剪切试验方法的基础上, 研制一种可实现现场测量焊接接头局部力学性能的新型装置, 双孔直径由原来的 2 mm 扩大至 6 mm, 提高了小桥区域测量的精度, 并借助有限元模拟, 建立双孔微剪切试验曲线与材料的强度的相关性. 这样不需要有限元计算, 直接通过双孔微剪切试验曲线得到材料的强度参数, 并对 X70 管线钢焊接接头的局部强度进行评定.

1 试验方法

双孔微剪切现场测量装置原理如图 1 所示. 首先, 利用自行设计的钻孔夹具装置在选定材料的被测区域的两侧钻直径为 6 mm, 深度为 3~5 mm 的两孔, 两孔间的小桥厚度为 0.3~0.5 mm, 为材料的被测区域. 通过定位小爪将装置固定, 施加力 F 于摆动杆, 摆动杆绕着与载荷传感器的接触处向右摆动, 压头从左侧孔对被测区域的材料加载, 使两孔之间的材料发生剪切变形直到断裂. 剪切速度由直流减速电机的转速控制. 位移传感器和载荷传感器记录加载过程中位移和载荷数据. 通过 LabVIEW 计算机软件控制部分得出相应的剪切载荷-位移曲线. 载荷除以剪切面积 A_0 得到名义剪切应力, $A_0 = 2hd + 0.168h + d + 0.0277$, 其中 h 为压头压入孔的深度, d 为两孔之间的小桥厚度. 位移除以剪切间隙

0.2 mm 得到名义剪切应变 γ .

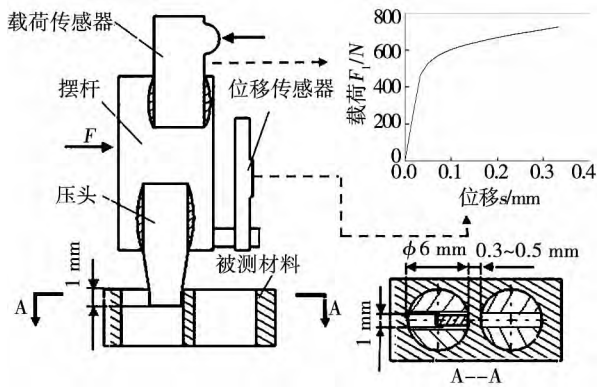


图1 双孔微剪切试验原理图

Fig. 1 Schematic of double holes micro-shear test

名义剪切应力应变曲线包含线弹性部分和塑性部分, 后者的表达式为

$$\tau = \tau_y (\gamma / \gamma_y)^{n_\tau} \quad (1)$$

式中: τ 是名义剪切应力; γ 是名义剪切应变; γ_y 和 τ_y 是屈服剪切应变和屈服剪应力; n_τ 是此幂函数的指数. 名义剪切应力-剪切应变曲线上弹性段的斜率取决于被测材料的弹性模量及双孔的几何尺寸, 对于同一类材料弹性模量变化很小, 弹性段的斜率变化不大, 方程中的屈服剪切应变可由屈服剪应力确定, 因此 τ_y 和 n_τ 是决定剪切应力-应变曲线塑性变形段的两个独立参量.

2 有限元方法

利用 ABAQUS 软件建立双孔微剪切试验的有限元模型. 用有限元分析力学性能不均匀的焊接接头的强度时, 不仅需要接头各部分材料的屈服应力, 而且还要提供材料屈服后的流变性能及抗拉强度. 用描述试样各部分的弹塑性变形行为的真应力应变曲线, 作为有限元计算的材料性能. 在有限元计算输入材料的性能时, 只将真应力应变曲线上真应力小于等于材料抗拉强度这部分数据输入. 并结合双孔微剪切试验所得到的曲线对有限元模型的参数进行调整, 对其精确度进行验证.

材料屈服后塑性变形的加工硬化过程符合幂函数规律, 其真应力应变曲线可描述为

$$\sigma = K \varepsilon^n \quad (2)$$

式中: $K = E^n \sigma_y^{n-1}$ 是强度系数; E 是弹性模量 206 GPa; σ 是真应力; ε 是真应变; σ_y 是屈服应力; n 是加工硬化指数. 屈服应力和加工硬化指数是反映材料的强度的两个基本参数.

利用 430 铁素体不锈钢作为试验材料进行常规

拉伸试验, 可得到其屈服应力为 $\sigma_y = 448$ MPa, 加工硬化指数 $n = 0.12$, 作为材料性能输入到双孔微剪切有限元模型中, 计算输出载荷位移曲线, 利用与剪切试验时所用的相同的处理方法, 得到剪切应力应变曲线. 在相同材料上进行双孔微剪切试验并做比较, 对有限元模型的参数进行调整, 如图 2 所示, 当调整模拟区域最小网格单元尺寸为 $0.15 \text{ mm} \times 0.05 \text{ mm} \times 0.05 \text{ mm}$ 时, 有限元分析结果与试验的剪切曲线基本是吻合的.

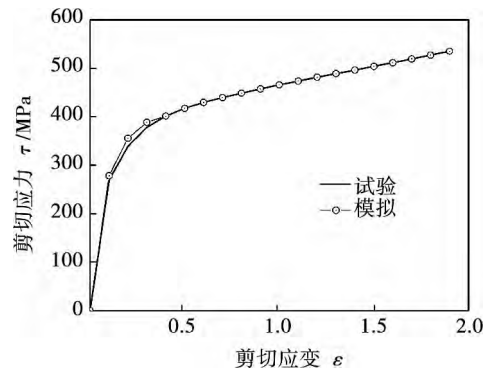


图2 双孔微剪切应力应变曲线与模拟对比

Fig. 2 Comparison of simulation and experiment curve

3 双孔微剪切曲线与材料强度参数的关系

建立屈服应力 σ_y 、加工硬化指数 n 与屈服剪应力 τ_y 、幂指数 n_τ 的相关性, 即可获得材料的强度参数和双孔微剪切试验曲线之间的关系. 首先假设一组材料性能, 屈服应力的取值为 200, 300, 400, 450, 500, 550 MPa, 加工硬化指数 n 的取值为 0.06, 0.08, 0.1, 0.12, 0.14, 0.16. 这些参数的范围基本上覆盖了常用的材料性能. 将屈服应力和加工硬化指数的 36 种不同的组合, 作为材料性能输入双孔微剪切试验的有限元模型进行有限元计算, 可得到对应 σ_y 和 n 的不同的组合系列剪应力剪应变曲线, 并从这些曲线得到相应特征参数屈服剪应力 τ_y 和指数 n_τ . 然后分析归纳材料性能参数 σ_y 和屈服剪应力 τ_y 的关系. 如图 3a 所示, 在加工硬化指数 n 值确定时, 屈服应力与屈服剪应力成线性关系. 其关系可以拟合为

$$\sigma_y = (1.757 - 1.996n) \tau_y + 85 \quad (3)$$

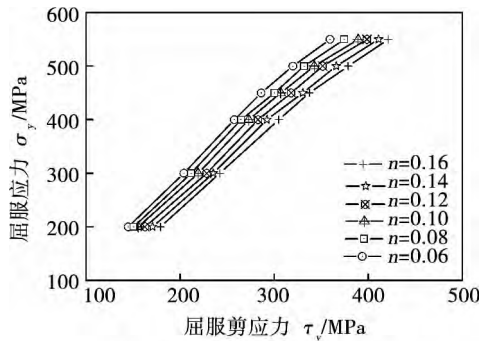
如图 3b 所示, 在 σ_y 值确定时, 加工硬化指数 n 和指数 n_τ 呈线性关系, 三者的关系可以拟合为

$$n = (1.32 - 3.12 \times 10^{-4} \sigma_y) n_\tau - 7.02 \times 10^{-5} \sigma_y - 0.077 \quad (4)$$

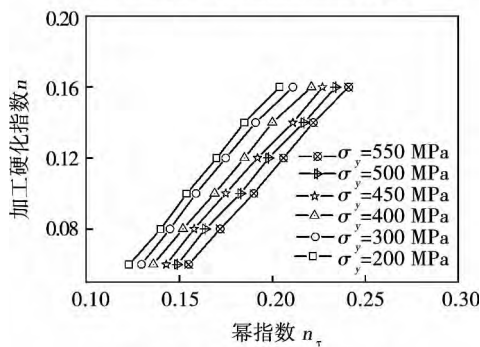
求解式 (3) 和式 (4) 得到

$$\sigma_y = \frac{2.635n_\tau\tau_y - 1.911\tau_y - 85}{6.236 \times 10^{-4}n_\tau\tau_y + 1.402 \times 10^{-4}\tau_y - 1} \quad (5)$$

$$n = \frac{5.48 \times 10^{-4}n_\tau\tau_y + 1.23 \times 10^{-4}\tau_y - 1.32n_\tau + 0.109}{6.236 \times 10^{-4}n_\tau\tau_y + 1.402 \times 10^{-4}\tau_y - 1} \quad (6)$$



(a) 屈服应力与屈服剪应力的关系



(b) 加工硬化指数与幂指数的关系

图 3 双孔微剪切试验曲线与材料塑性变形参数的关系

Fig. 3 Relationship between double hole microshear test curve and plastic deformation parameters

利用双孔微剪切试验的载荷位移曲线,根据式(5)和式(6)直接得到材料的强度参数.

将 X70 管线钢母材作为试验材料进行拉伸和双孔微剪切试验对上述关系进行验证. 对 X70 管线钢母材进行双孔微剪切试验,通过双孔微剪切现场测试系统转化的名义剪切应力 - 应变曲线直接得出三组屈服剪应力 τ_y 和指数 n_τ 数据,屈服强度 R_{eLy} 和加工硬化指数 n^* 可通过式(5)和式(6)得到. 同时对同种材料拉伸试验得到 X70 管线钢的工程应力 - 应变曲线. 拉伸试验的抗拉强度是试样发生颈缩时的名义应力,颈缩的发生与变形过程中材料的加工硬化性能有关;屈服强度用引起 0.2% 塑性变形的名义应力来确定,对于加工硬化过程符合幂函数规律的材料的拉伸试样,最大载荷处的真应变等于材料的加工硬化指数 n . 从而获得拉伸屈服应力 σ_y 和加工硬化指数 n . 如表 1 所示. 与 R_{eLy} 相对误差不大于 1.5%; n^* 与 n 的相对误差不大于 6.6%. 由此可以认为选择不同屈服应力和加工硬化指数的材料进行有限元模拟,所得到的双孔微剪切试验曲线与材料强度参数的关系式是可信的.

4 X70 管线钢焊接接头局部强度评定

利用双孔微剪切试验对 X70 管线钢焊接接头的强度进行评定. 焊接试板取自国内某钢厂生产的低碳微合金控轧 X70 管线钢轧制板,板厚为 14.8 mm,焊接接头的坡口为 U 形,采用焊接带约束电弧超窄间隙进行焊接,焊丝为 H08Mn2Si,焊剂带的主要成

表 1 剪切试验与拉伸试验结果比较

Table 1 Comparison between shear test and tensile test results

屈服剪应力 τ_y /MPa	幂指数 n_τ	加工硬化 (剪切) 指数 n^*	屈服强度 R_{eLy} /MPa	屈服应力 σ_y /MPa	加工硬化指数 (拉伸) n	屈服强度误差 $(R_{eLy} - \sigma_y) / R_{eLy} (\%)$	加工硬化指数误差 $(n^* - n) / n (\%)$
275.7	0.148	0.056	538.76	545.57	0.057	1.2	1.7
269.8	0.138	0.045	534.56	540.11	0.048	1.0	6.6
279.6	0.139	0.060	542.62	551.04	0.062	1.5	2.4

分为萤石和大理石,接头为多层焊接接头(共 4 层). 如图 4 所示,在焊接接头上选择距离焊缝不同距离的点为被测点,在每个被测点两侧沿垂直于焊缝的方向钻双孔,相邻双孔之间的距离为 5 mm,进行双孔微剪切试验.

利用双孔微剪切现场测试装置进行试验,得出 X70 管线钢焊接接头的剪切载荷 - 位移曲线,从而得到屈服剪应力 τ_y 和指数 n_τ . 利用式(5)和式(6)进行转换,可得到屈服应力 σ_y 和加工硬化指数 n 在接头上的分布,利用文献 [9] 中给出的加工硬化指

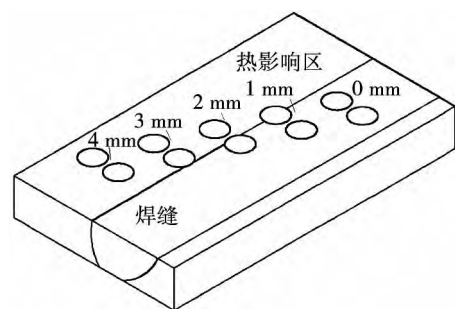


图 4 剪切孔的分布

Fig. 4 Distribution of shear hole

数和屈服强度及抗拉强度的相关公式,计算得到相对应抗拉强度值.利用传统硬度试验获得接头各区维氏硬度值,图5为X70管线钢焊接接头的强度和硬度(HV)分布.可以看出,焊缝区及热影响区的屈服强度、抗拉强度值均低于母材区,其强度分布与硬度分布相似.接头属于低匹配.热影响区加工硬化指数明显降低,并出现最低值.

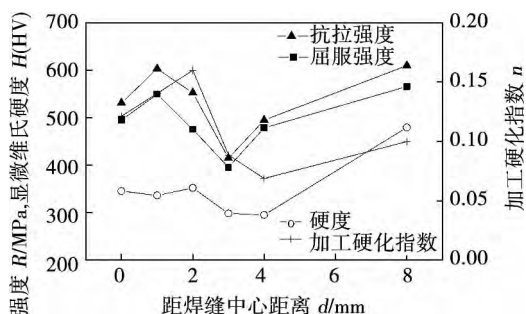


图5 焊接接头强度与加工硬化指数和硬度分布

Fig. 5 Distribution of R , n and HV with X70 pipeline steel welded joint

5 结 论

(1) 研制双孔微剪切试验装置,用来评定焊接接头局部力学性能.

(2) 提出了根据双孔微剪切试验曲线确定材料强度的方法.利用有限元模拟,给出了材料强度参数与试验载荷位移曲线的相关关系,其准确性用拉伸试验得到了验证.

(3) 测定 X70 管线钢焊接接头的局部强度分布趋势.焊接接头焊缝区和热影响区的强度值均低于母材区域,其分布与硬度分布相似.加工硬化指数在焊缝区出现高峰,热影响区加工硬化指数值相对较低.

参考文献:

- [1] 朱亮,陈剑虹.热影响区软化焊接接头应力分布特征及强度预测[J].焊接学报,2004,25(3):61-65.
Zhu Liang, Chen Jianhong. Characteristics of stress distribution

and prediction of strength in heat affected zone softened welded joints[J]. Transactions of the China Welding Institution, 2004, 25(3): 61-65.

- [2] 史耀武,周宁宁,张新平,等.微剪切试验及对焊接接头力学性能的评价[J].焊接学报,1994,15(4):235-240.
Shi Yaowu, Zhou Ningning, Zhang Xinping, et al. Microshear test and its evaluation to mechanical properties of welded joints [J]. Transactions of the China Welding Institution, 1994, 15(4): 235-240.
- [3] Umekuni A, Masubuchi K. Usefulness of under matched welds for high-strength steels [J]. Welding Journal, 1997, 76(7): 256-263.
- [4] Asif Husain, Sehgal D K, Pandey R K. An inverse finite element procedure for the determination of constitutive tensile behavior of materials using miniature specimen [J]. Computational Materials Science, 2004, 31(1-2): 84-92.
- [5] 雷斌隆.评定铝合金焊接接头力学性能的新途径[J].机械工程材料,2004,28(4):13-15.
Lei Binlong. A new way of mechanical properties of welded joints in evaluation of aluminum alloy [J]. Mechanical Engineering Materials, 2004, 28(4): 13-15.
- [6] LaVan D A. Microtensile properties of weld metal [J]. Experimental Techniques, Wilson Applied Science & Technology Abstracts, 1999, 23(3): 30-34.
- [7] Zhang X P, Dorn L. Estimation of the local mechanical properties of pipeline steels and welded joints by use of the micro shear test method [J]. International Journal of Pressure Vessels and Piping, 1998, 75(4): 37-42.
- [8] 朱亮,任国松,龙林,等.双孔微剪切测定铝合金焊接接头的局部本构特性[J].材料工程,2007(10):18-22.
Zhu Liang, Ren Guosong, Long Lin, et al. Determination of local constitutive properties of welded joints in aluminum alloy using double holes micro shear test [J]. Journal of Materials Engineering, 2007(10): 18-22.
- [9] 朱亮,陈剑虹.力学性能不均匀焊接接头的强度预测[J].焊接学报,2005,26(3):48-51.
Zhu Liang, Chen Jianhong. Prediction of tensile properties of welded joint with mechanical heterogeneity [J]. Transactions of the China Welding Institution, 2005, 26(3): 48-51.

作者简介:蔡淑娟,女,1980年出生,博士研究生.主要从事焊接接头的力学性能方面的研究.发表论文5篇. Email: lanney1203@163.com

通讯作者:朱亮,男,教授,博士研究生导师. Email: zhul@lut.cn

tool is more significant than increasing the refill velocity. These conclusions by simulation were verified by the experiment.

Key words: refill friction stir spot welding; numerical simulation; material flow; refill velocity

Evaluation of local strength of welding joint by using double holes micro shear test

CAI Shujuan, ZHU Liang, ZHANG Zhongfa (State Key Laboratory of Advanced Processing and Recycling of Nonferrous Metals, Lanzhou University of Technology, Lanzhou 730050, China). pp 43 – 46

Abstract: A new approach, double holes micro shear test, is presented for determining the local plastic deformation properties in welded joints. A device for measuring the local mechanical properties of materials is developed and the micro shear test of the welded joint is carried out. The response between applied load and indenter displacement is recorded. Shear stress-strain curve, the finite element model of double hole micro-shear test is established. The finite element computation were carried out for various combination of yield stress and work hardening exponent. The equations were constructed to material strength properties and load-displacement curves from double holes micro-shear tests. The accuracy of this equations method is validated by tensile test. The results show that the material strength properties can be obtained directly from the experimental curves with double hole micro-shear test. The local distortion properties in X70 pipeline steel welded joints were evaluated by double holes micro shear test.

Key words: double hole micro-shear test; finite element simulation; yield stress

Joining of SiO₂/SiO₂ composite to Nb using Ag-Cu-In-Ti brazing filler

CHEN Bo, WU Shibiao, XIONG Huaping, LI Wenwen (Welding and Plastic Forming Division, Beijing Institute of Aeronautical Materials, Beijing 100095, China). pp 47 – 51

Abstract: A novel Ag-(15 ~ 26)Cu-(13 ~ 20)In-(3.1 ~ 6.9)Ti active filler alloy was designed for joining of SiO₂/SiO₂ composite to Nb at 780 °C for 20 min, 780 °C for 40 min and 800 °C for 10 min, respectively. The joints brazed with the filler alloy at 800 °C for 10 min presented the maximum average shear strength of 21.6 MPa. During the brazing process, the active element Ti diffused significantly from the Ag-Cu-In-Ti alloy to the surface of the SiO₂/SiO₂ composite and a thin reaction layer with a thickness of 2 μm was formed close to the composite. Sound interface was also obtained between the filler alloy and Nb. The interface structure of the joint brazed with Ag-(15 ~ 26)Cu-(13 ~ 20)In-(3.1 ~ 6.9)Ti alloy can be described as the following sequence: SiO₂/SiO₂ → TiO + TiSi₂ → TiO + Cu₃Ti → Ag(s, s) + Ag₃In + Cu(s, s) → Nb.

Key words: SiO₂/SiO₂ composite; Nb; brazing; reaction layer; shear strength

Impact of external magnetic field generated by permanent magnet on mechanical property and microstructure of aluminum alloy resistance spot weld

YAO Qi^{1,2}, LI Yang^{1,2}, LUO Zhen^{1,2}, ZHANG Yu^{1,2} (1. School of Materials Science and Engineering, Tianjin University, Tianjin 300072, China; 2. Collaborative Innovation Center of Advanced Ship and Deep-Sea Exploration, Shanghai 200240, China). pp 52 – 56

Abstract: This paper systematically analyze the effect of external magnetic field (EMF) generated by permanent magnetic on the nugget size, mechanical properties and failure mode of aluminum alloy resistance spot welds. The relationship between nugget size and peak load was also studied. The results show that the work distance between two permanent magnets has significant effect on the nugget diameter. The smaller the distance is, the larger the nugget diameter is. The nugget diameter and tensile-shear force were increased under the help of EMF. Under different welding parameters, the nugget diameter can be increased by 3.5% ~ 14.1%, and the tensile-shear force enhanced 4 ~ 25%. The EMF promotes the failure mode change from interfacial failure to pullout failure. The EMF can improve the strength-toughness properties and refine grain size. The relationship between peak load and the product of nugget diameter, workpiece thickness and base material ultimate tensile strength shows well linear relation.

Key words: resistance spot welding; external magnetic field; aluminum alloy; mechanical property; failure mode

Effect of hydrogenation on uniformity of superplastic deformation of titanium alloy laser weld

FAN Zhao, CHENG Donghai, CHEN Yiping, HU Dean (School of Materials Science and Engineering, Nanchang Hangkong University, Nanchang 330063, China). pp 57 – 60

Abstract: Hydrogenation can improve the uniformity of superplastic deformation of TC4 titanium alloy laser weld. The non-uniform deformation coefficient K was introduced to quantitatively characterize the non-uniform deformation. The results indicate that when the hydrogen content exceeded 0.2%, the superplastic property of welded joint degraded with the increase of hydrogen, with increase of peak flow stress and decrease of percentage reduction in area, but the uniformity of superplastic deformation increased. With the increasing of hydrogen content, the percentage reduction in area of base metal decreased more than that of welded joint. The non-uniform deformation coefficient K can characterize the non-uniform deformation of the titanium alloy laser weld and base materials with hydrogenation during superplastic deformation. The K value increased with the increase of hydrogen content, the increase of temperature, and the decrease of strain rate. The K value reached the maximum value 0.84 when the hydrogen content was 1.299%, the deformation temperature was 920 °C, and the strain rate was 10⁻⁴ s⁻¹.

Key words: hydrogenation; laser welding; non-uniform deformation; superplastic

Critical width of tensile-shear test specimen for resistance spot welding joints

CUI Xuetao¹, ZHAO Yujin^{1,2}, LUO Zhen¹, YAN Fuyu¹, AO Sansan¹, LUO Tong³ (1. School of Materials Science and Engineering, Tianjin University, Tianjin 300072, China; 2. Department of Mechanical Engineering, University of South Carolina, Columbia 29208, China; 3. Detection Center of Natural Gas Branch Company of Daqing Oil Field, Daqing 163000, China). pp 61 – 64

Abstract: It is found that the standard of shear tensile test of resistance spot welding is not uniform. The material used was galvanized Q235 stainless steel. The trend of failure load, failure displacement and energy absorption with the change of the width of the specimen were detected. The reasons for this change